Effect of Electrode Geometry and Charge on the Production of Polymer Microbeads by Electrostatics

B. BUGARSKI[1], B. AMSDEN[1], R. J. NEUFELD[2], D. PONCELET[2] and M. F. A. GOOSEN[1]*

[1]Department of Chemical Engineering, Queen's University, Kingston, Ontario K7L 3N6
[2]Department of Chemical Engineering, McGill University, Montreal, Quebec H3A 2A7

Experimental parameters which are critical for producing small diameter (i.e. 100–300 μm) polymer microbeads, using electrostatic droplet generation, were investigated with three types of electrodes; a parallel plate, a positively charged needle and a grounded needle with alginate as the polymer. Electrode spacing was a critical factor controlling microbead size, but only for the parallel plate set-up. While the applied potential affected droplet size in all three set-ups, the smallest droplet size was produced with the positively charged needle. In some experiments needle oscillation was observed resulting in even smaller microbeads (i.e. < 100 μm). Calculated microbead diameters agreed well with experimental values.

Des paramètres expérimentaux critiques pour la production de microbilles de polymère de petits diamètres (p.ex. 100–300 μm), par la génération de gouttelettes électrostatiques, ont été étudiés avec trois types d'électrodes: un plateau parallèle, une aiguille chargée positivement et une aiguille mise à la terre avec de l'alginate comme polymère. L'espacement des électrodes est un facteur critique régulateur de la taille des microbilles, mais uniquement pour le montage à plateaux parallèles. Alors que le potentiel appliqué influence la taille des gouttelettes dans les trois montages, la taille la plus petite a été obtenue avec l'aiguille chargée positivement. Dans certaines expériences, on a observé une oscillation de l'aiguille qui a entrainé la formation de microbilles encore plus petites (< 100 μm). Les diamètres de microbilles calculés montrent un bon accord avec les valeurs expérimentales.

Keywords: electrostatics, droplet-generation, microbead, modelling, scale-up.

There has been a great deal of interest over the years in the behavior of conducting liquid drops immersed in electric fields (Nawab and Mason, 1958; Balachandran and Bailey, 1984; Fillimore and Lokeren, 1982; Goosen et al., 1986). The formation of an electrostatic spray, for example, can be observed by gradually applying a potential to a capillary through which a liquid is flowing at a relatively low flow rate. The motivation for these electrostatic studies has arisen from a wide diversity of scientific and engineering applications of this technology, including ink jet spraying, separation and dielectrophoresis.

The primary objective of this paper was to investigate the experimental parameters which are critical for producing small diameter (i.e. 100–300 μm) polymer microbeads using electrostatic droplet generation. Specifically, electrode geometry, applied voltage, charge polarity, electrode spacing and needle size were investigated. Furthermore, the optimum conditions for the production of small uniform polymer beads using three types of electrodes; a parallel plate, positively charged needle, and a grounded needle were assessed.

Analysis of forces acting on a droplet in an electric field

In the absence of an applied voltage, a liquid drop falls from the end of a capillary tube at a critical drop volume dependent on the surface tension (i.e., the liquid drop would continue to grow until its mass overcomes the surface tension). If gravity were the only force acting on the meniscus of the droplet, large uniformly sized droplets would be produced with a radius r. Equating the gravitational force on the droplet to the capillary surface force gives:

$$r = (3r_o\gamma/2\rho g)^{1/3} \quad \ldots\ldots (1)$$

where r_o is the internal radius of the needle, γ is the surface tension, ρ is the relative density of the polymer solution and g is the acceleration constant.

Under the action of an electric field, the electric force F_e, acting along with the gravitational force, F_g, would reduce the critical volume for drop detachment resulting in a smaller droplet diameter. Equating the gravitational and electrical forces on the droplet to the capillary surface force yields:

$$F_\gamma = F_g + F_e \quad \ldots\ldots (2)$$

Three electrode geometries were considered; (1) a parallel plate arrangement in which the charge was applied to a plate held parallel to the collecting solution and through the centre of which the needle protruded (Figure 1A); (2) having the needle alone with the charge applied directly to the collecting solution (Figure 1B); and (3) applying the charge to a solitary needle (Figure 1C).

In the case of a parallel plate electrode set up (Figure 1A) the electrostatic force exerted on a needle was found by modifying the expression obtained by Taylor (1966):

$$F_e = \pi\epsilon_o V^2 L^2 / H^2 \, [\ln(2L/r_o) - 3/2] \quad \ldots\ldots (3)$$

in which L is the height of the needle in the electric field, H is the electrode distance , V is the applied voltage, and ϵ_o is the permittivity of the air.

In the case of a charged needle (Figure 1C), the stress produced by the external field at the needle tip is obtained using a modified expression developed by DeShon and Carlson (1968):

$$F_e = 4\pi\epsilon_o V^2 / [\ln(4H/r_o)]^2 \quad \ldots\ldots (4)$$

Substituting Equation (3) into Equation (2) results in a relationship describing the effect of the applied potential on the droplet radius for the parallel plate arrangement:

*Author to whom correspondence should be addressed.

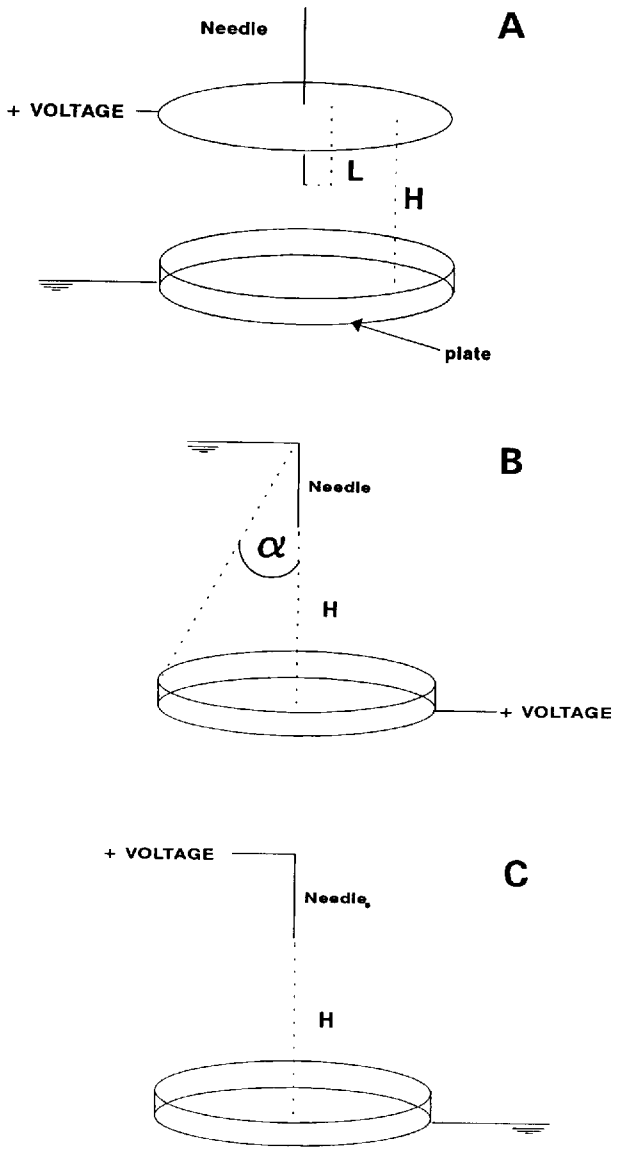

Figure 1 — Electrode and charge arrangements; A: Parallel plate set-up with positively charged plate; B: Positively charged collecting plate; C: Positively charged needle.

$$r = \{[3/4\ \rho g]\ [r_o\gamma - (\epsilon_0 V^2 L^2)\ /\ (H^2[\ln(2L/r_o) - 3/2])]\}^{1/3} \quad \ldots\ldots\ldots\ldots\ldots\ldots \quad (5)$$

Similarly, the effect of applied potential on the droplet radius for the charged needle arrangement can be derived by substituting Equation (4) into (2):

$$r = ([3/2\ \rho g]\ [r_o\gamma - (2\epsilon_0 V^2)\ /\ (\ln(4H/r_o))])^{1/3} \quad \ldots \quad (6)$$

For the positively charged collecting plate and grounded needle (Figure 1B) an empirical relationship was obtained from the expression given by Hommel et al. (1988).

$$r = \{[3/2\ \rho g]\ [r_o\gamma - (\epsilon_0 V^2 4\cos(\alpha))\ /\ H]\}^{1/3} \quad \ldots\ldots \quad (7)$$

in which α is the angle defined in Figure 1B.

The last three equations can be used to calculate the droplet size as a function of applied voltage for the three electrode geometries studied.

Materials and Methods

CHEMICALS

Sodium alginate (Protanal LF 20/60) with a viscosity of 150-200 mPa/s was purchased from Protan (North Hampton, U.S.A.). Calcium chloride was obtained from BDH (Toronto, Ontario). 22 and 26 gauge needles (H80763, H80429) were purchased from Chromatographic Specialties Inc. (Brockville, Ontario).

ELECTROSTATIC DROPLET GENERATION

The droplets were formed by extruding an alginate/water solution through either a 22 or 26 gauge needle using a syringe pump. The needle tip-to-collecting solution (1.5% $CaCl_2$) distance was maintained at either 2.5, 3.5, or 4.8 cm. The applied potential was varied between 0 and 25 kV using a direct current power supply (Model 30R, Betran Associates Inc., Ont.).

DETERMINATION OF MIRCROBEAD SIZE DISTRIBUTION BY LASER LIGHT SCATTERING

Volumetric (volume of microspheres in each diameter class) and cumulative size distributions were determined by laser light scattering, using a 2602-LC particle analyzer (Malverin Instruments, NY) according to the log-normal distribution model. The mean diameter and the arithmetic standard deviation were calculated from the cumulative distribution curve (Poncelet et al., 1989).

INVESTIGATION OF DROPLET FORMATION MECHANISM USING IMAGE ANALYSIS

The mechanism of droplet formation was also examined. A video camera (Sony, CCD, Japan) was connected to a microscope lens (Olympus SZH, Optical Co. Ltd., Japan) (Figure 3). Droplet formation under the infuence of electrostatic forces was then observed with a stroboscopic light at a defined frequency. The images were recorded and compared when the frequencies of light flashes and droplet formation were identical so that the object appeared to be 'frozen'. A sample containing 50 to 150 beads (after hardening for 15 minutes in the $CaCl_2$ solution) was taken from each set of experiments. The diameter of the individual beads was measured under a microscope using a video Image Analysis program (Java, Jandel Scientific, Corte Madera, CA).

Results and discussion

EFFECT OF ELECTRODE GEOMETRY, CHARGE ARRANGEMENTS, APPLIED POTENTIAL AND ELECTRODE SPACING

The effect of applied potential and electrode spacing for the parallel plate set-up on polymer microbead diameter is shown in Figure 2A. As the potential between the electrodes increased from 2 to 12 kV, the average bead diameter decreased from 2500 to 350 μm. Reducing the electrode distance resulted in smaller microbread diameters, suggesting a strong influence of distance and voltage on bead size with the parallel plate electrode arrangement. For example, at a potential difference of 8 kV, reducing the distance from 4.8 to 2.5 cm resulted in a decrease in polymer bead size from 2200 to 700 μm. Increasing the potential above 12 kV and decreasing the electrode spacing below 2.5 cm did not result in smaller bead diameters. This was probably due to

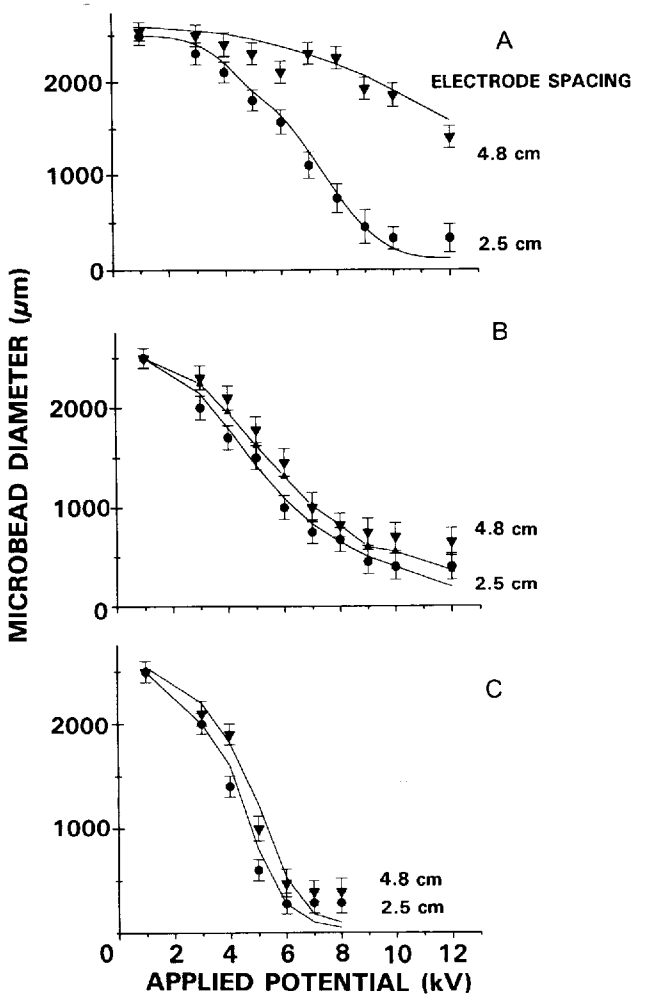

Figure 2 — Effect on microbead size of applied potential and electrode spacing; A: parallel plate set-up; B: Positively charged collecting plate; C: Positively charged needle. Alginate concentration 1.5%, 22 gauge needle in all three configurations.

electrostatic discharge between the plates, accompanied by sparking, as a result of air ionization in the space between the electrodes.

With the positively charged plate and grounded needle configuration (Figure 1B), reducing the electrode distance from 4.8 cm to 2.5 cm at 8 kV resulted in only a moderate decrease in bead diameter from 800 to 600 μm (Figure 2B).

In the last set-up (Figure 1C), the same electrode geometry was employed as in the previous case, but with reversed polarity (i.e. positively charged needle). The electrode spacing in this case also had very little effect on microbead diameter. For example, when the electrode distance was reduced from 4.8 to 2.5 cm at a potential difference of 8 kV, the microbead diameter decreased only slightly from 380 to 330 μm. Furthermore, microbead diameter was unaffected by an applied potential above 6 kV, due presumably to charge build-up in the vicinity of the needle.

Further reduction in microbead size was achieved by decreasing the needle size from 22 to 26 gauge (Figure 3). The same general trend was observed with all three geometries examined. Droplet diameter decreased with increasing voltage and then leveled off. It is interesting to note that a decrease of 10–50% in microbead diameter was observed when going to the smaller needle size (26 gauge)

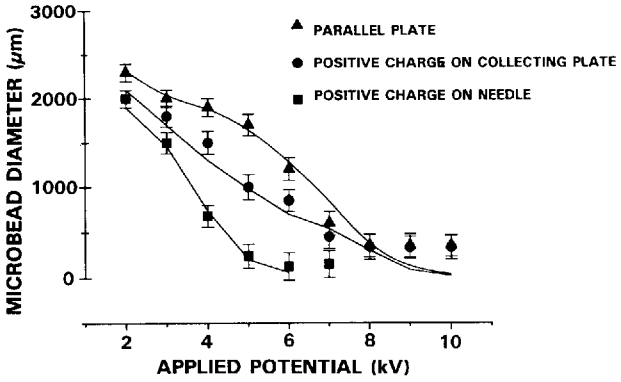

Figure 3 — Effect on microbead diameter of applied potential for all three electrode set-ups.

with all three charge arrangements. Above 8 kV a moderate decrease of only 10% was observed with the parallel plate set-up, when going from a 22 to a 26 gauge needle. Similarly, with a positively charged plate the mean bead diameter decreased from 600 to 400 μm, at the same applied potential of 8 kV when going to the smaller needle. The greatest decrease was observed with a positively charged needle, where at 8kV the minimum bead diameter decreased from 270 to about 150 μm when going from a 22 to a 26 gauge needle. When a sufficiently high charge was added to the droplet (i.e. applied potential above 8 kV), detaching droplets did not have enough time for break-up due to the higher velocity of droples induced by a more intense electric field (i.e. they were forced into the hardening solution and gelled before break-up). As a result, a further increase in applied potential did not result in reduction in droplet size.

A comparison was made between the measured and calculated droplet/microbead diameters (Figures 2 and 3). The general shapes of the calculated curves were similar to those of the experimental curves. Very good agreement between experimental and calculated data was achieved with the 22 gauge needle in all three charge configurations. The calculated droplet diameter, for the range of applied potentials studied (2-12 kV), agreed well with the experimental data with an error of $\pm$ 15%. Equally successful was the agreement for the 26 gauge needle, where the calculated and experimental data agreed within an error of $\pm$ 10%.

INVESTIGATION OF MECHANISM OF DROPLET FORMATION BY IMAGE ANALYSES

Comparative studies of the three electrode geometries at the same applied potential and needle size were carried out in order to give an insight into the droplet formation mechanism. Looking at the formation of the droplet at the needle tip using an image analysis/video system, at the same potential difference (6 kV), needle size (26 gauge), electrode spacing (2.5 cm) and flow rate (0.036 L/h), we observed a different droplet diameter for each electrode geometry and charge arrangement. For the parallel plate, the frequency of droplets leaving the tip of the needle was below that required to initiate spraying (i.e. liquid jet formation). The average bead diameter was found to be 1150 $\pm$ 200 μm. With the positive charge on the collecting plate arrangement, a much higher frequency of forming droplets was observed with an average bead diameter of 600 $\pm$ 100 μm. Finally, with the positively charged needle arrangement, a well developed

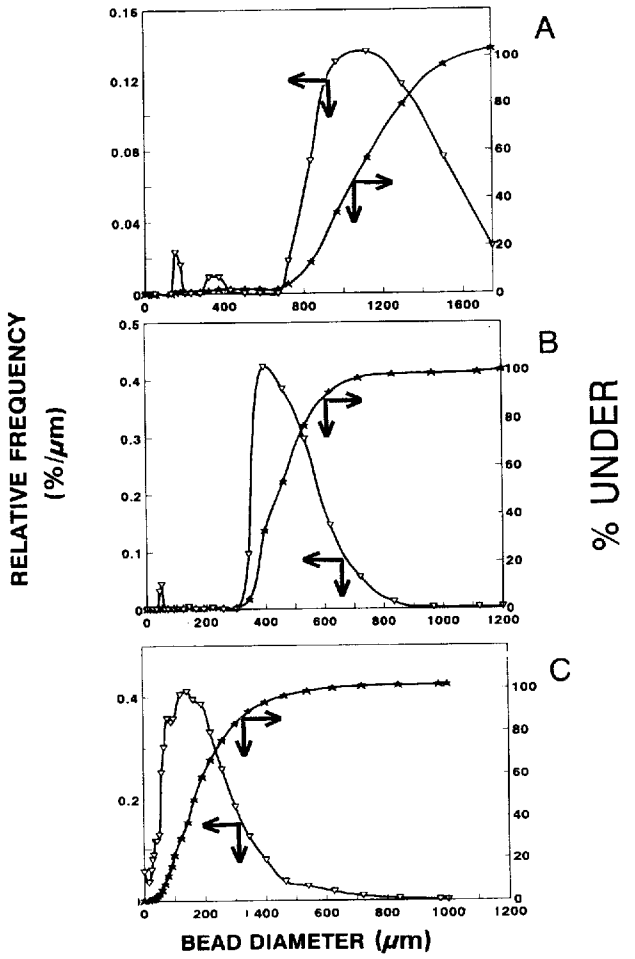

Figure 4 — Droplet size distribution previously produced with, A: Parallel plate, B: Positively charged collecting plate, and C: Positively charged needle at the same potential (6KV) and electrode distance of 2.5 cm.

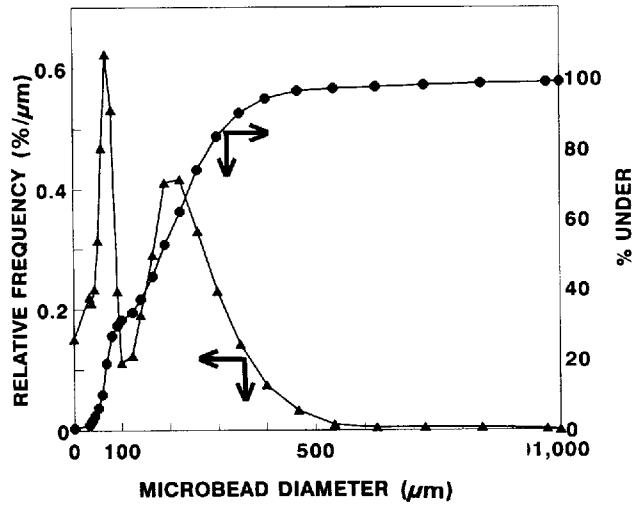

Figure 5 — Droplet size distribution produced with positively charged 26 g. needle, 2.5 cm electrode distance, at 6.5 KV.

liquid jet or spraying (80 μm in diameter) was observed at the end of a Taylor-like meniscus (Taylor, 1966), giving droplets of 150 $\pm$ 70 μm in diameter.

The mean bead size distribution curves obtained by plotting relative frequencies versus bead diameter, typically resulted in a continuous function symmetrical about the mean value. At 6 kV, the mean bead size distribution was found to vary about the mean of 1150 μm (Figure 4A) and 430 μm (Figure 4B) and 150 μm (Figure 4C) for the parallel plate, positively charged collecting plate and positively charged needle, respectively.

As the voltage increased above 6kV, with the positively charged 26 needle, harmonic oscillation of the needle was observed. This periodic oscillation of the electrically stressed meniscus at the capillary tip caused distortion of the single liquid jet resulting in a whipping action of the oscillating thread-like filament. At 6.5 kV a bimodal bead size distribution was observed, one peak at 50 μm and a second peak at 160 μm (Figure 5). This needle oscillation phenomenon was not observed with the other two charge arrangements.

Analysis of Electric Field and Surface Charge

As the voltage increased beyond a critical point (known as the minimum spraying potential), a transition from the dripping mode, where individual droplets could be seen to come off the end of the needle, to a high frequency spraying mode (i.e. liquid jet) was observed with all three charge arrangements. The minimum spraying potential for the positively charged needle set-up was observed to be lower than that for the parallel and charged plates. The process of droplet formation suggests that the forces due to the presence of an external electric field and the surface charge are responsible for the instability of the droplets at the needle tip. The charges which are distributed on the liquid surface repel each other and cause a force opposing the surface tension. In the case of the positively charged needle, the conducting liquid and needle are in the close contact bearing approximately the same potential difference (Sample and Bollini, 1972). The electric field (E) at the meniscus is therefore proportional to the applied voltage, V, and radius of the meniscus, r_o. The area over which the surface charge operates varies with $1/r^2$. Due to the small area available for charge distribution (the needle tip) the overall surface charge would be higher for this electrode arrangement, than for the two other set-ups at the same potential difference. For the parallel plate set-up, the uniform electric field between the two electrodes was proportional to the potential difference and electrode spacing, H. Therefore, a much higher potential difference was required to build a sufficiently large charge on the plate to initiate spraying (i.e. 8 kV for the parallel plate versus 5 kV for the positive needle set-up).

The positively charged plate, with grounded needle, is the reverse arrangement of the positively charged needle. Results with this geometry show that the reversed polarity had an impact on bead size with the charged plate set-up giving smaller bead sizes. This may be due to the larger area over which the surface charge has to spread (i.e the area of the hardening solution, $CaCl_2$). In this situation the charge density on the forming drop would be lower than in case of a positively charged needle, where the charge area was limited to the liquid meniscus at the needle tip. The net effect being a weaker force pulling the droplet from the tip of the needle.

Conclusions

Electrode spacing was a critical factor in controlling microbead size for the parallel plate set-up, but not for the positively charged collecting plate and the positively charged needle arrangements. While the applied potential affected droplet size in all three electrode set-ups, the smallest droplet size was produced with the positively charged small diameter needle due to the high surface charge and intense electric field in the vicinity of the needle tip. With the 26 gauge needle, needle oscillation was observed resulting in a significant fraction (30% by volume) of very small (50 μm) microbeads. Calculated microbead diameters agreed very well with experimentally determined values.

Nomenclature

E = electric field, V/m
F_e = electrostatic force, N
F_g = gravitational force, N
F_γ = surface tension force, N
g = gravitational constant, m/s^2
H = electrode distance, m
L = length of needle in electric field between electrodes, m
q = electric charge, C
r = radius of the forming droplet, m
r_o = internal radius of the needle

Greek letters

α = angle defined in Figure 1B
γ = surface tension, N/m
ρ = density, kg/m^3

References

Balachandran, W. and A. G. Bailey, "The Dispersion of Liquids Using Centrifugal and Electrostatic Forces", *IEEE Trans. Ind. App.*, IA20, 682-686 (1984).

DeShon, E. W. and R. Carlson, "Electric Field and Model for Electrical Liquid Spraying" *J. Colloid Sci.* **28**, 161-166 (1968).

Fillimore, G. L. and D. C. Van Lokeren, "Multinozzle Drop Generator Which Produces Uniform Break up of Continuous Jets", Proc. *IEEE Ann. Meeting of the Industrial Society* (1982), pp. 991-998.

Goosen, M. F. A., G. M. O'Shea, M. M. Gharapetian and A. M. Sun. "Immobilization of Living Cells in Biocompatible Semi-permeable Microcapsules: Biomedical and Potential Biochemical Engineering Applications", in "Polymers in Medicine", E. Chiellini, ed., Plenum Publ. Co., New York (1986), p. 235-246.

Hommel, M., A. M. Sun and M. F. A. Goosen, "Droplet Generation", Canadian Patent 1,241,598 (1988).

Nawab, M. A. and S. G. Mason, "The Preparation of Uniform Emulsions by Electrical Dispersion", *J. Colloid Sci.* **13**, 179-187 (1958).

Poncelet, B., D. Poncelet and R. J. Neufeld, "Control and Mean Diameter and Size Distribution During Formulation of Microcapsules with Cellulose Nitrate Membranes", *Enzyme Microbiol. Technol.* **11**, 29-37 (1989).

Sample, S. B., and R. Bollini, "Production of Liquid Aerosols by Harmonic Electrical Spraying", *J. Colloid. Sci.* **14**, 185-193 (1972).

Taylor, G.I., "The Force Exerted by an Electric Field on Long Cylindical Conductors", *Proc. Roy. Soc. A* **291**, 145-152 (1966).

Manuscript received June 11, 1993; revised manuscript received February 9,1994; accepted for publication February 11, 1994.